JOURNAL OF BACTERIOLOGY, Apr. 2006, p. 2919–2927 Vol. 188, No. 8
0021-9193/06/$08.00+0 doi:10.1128/JB.188.8.2919–2927.2006

Aerobic Benzoyl-Coenzyme A (CoA) Catabolic Pathway in *Azoarcus evansii*: Conversion of Ring Cleavage Product by 3,4-Dehydroadipyl-CoA Semialdehyde Dehydrogenase

Johannes Gescher,[1] Wael Ismail,[1] Ellen Ölgeschläger,[1] Wolfgang Eisenreich,[2] Jürgen Wörth,[3] and Georg Fuchs[1]*

Mikrobiologie, Institut für Biologie II, Universität Freiburg, Freiburg, Germany[1]; Lehrstuhl für Organische Chemie und Biochemie, Technische Universität München, Munich, Germany[2]; and Institut für organische Chemie und Biochemie, Fakultät für Chemie, Universität Freiburg, Albertstr. 21, D-79104 Freiburg, Germany[3]

Received 14 December 2005/Accepted 27 January 2006

Benzoate, a strategic intermediate in aerobic aromatic metabolism, is metabolized in various bacteria via an unorthodox pathway. The intermediates of this pathway are coenzyme A (CoA) thioesters throughout, and ring cleavage is nonoxygenolytic. The fate of the ring cleavage product 3,4-dehydroadipyl-CoA semialdehyde was studied in the β-proteobacterium *Azoarcus evansii*. Cell extracts contained a benzoate-induced, $NADP^+$-specific aldehyde dehydrogenase, which oxidized this intermediate. A postulated putative long-chain aldehyde dehydrogenase gene, which might encode this new enzyme, is located on a cluster of genes encoding enzymes and a transport system required for aerobic benzoate oxidation. The gene was expressed in *Escherichia coli*, and the maltose-binding protein-tagged enzyme was purified and studied. It is a homodimer composed of 54 kDa (without tag) subunits and was confirmed to be the desired 3,4-dehydroadipyl-CoA semialdehyde dehydrogenase. The reaction product was identified by nuclear magnetic resonance spectroscopy as the corresponding acid 3,4-dehydroadipyl-CoA. Hence, the intermediates of aerobic benzoyl-CoA catabolic pathway recognized so far are benzoyl-CoA; 2,3-dihydro-2,3-dihydroxybenzoyl-CoA; 3,4-dehydroadipyl-CoA semialdehyde plus formate; and 3,4-dehydroadipyl-CoA. The further metabolism is thought to lead to 3-oxoadipyl-CoA, the intermediate at which the conventional and the unorthodox pathways merge.

The pathways of aerobic metabolism of benzoate generally follow a well-established strategy for aerobic aromatic metabolism (Fig. 1A) (10, 19). They include hydroxylation of the aromatic ring by monooxygenases or dioxygenases, whereby catechol (1,2-dihydroxybenzene) or protocatechuate (3,4-dihydroxybenzoate) is produced. These central aromatic intermediates are the substrates for ring-cleaving dioxygenases (5, 6). The classical β-ketoadipate pathway (*ortho* cleavage of the ring) leads to β-ketoadipate, which is subsequently converted to succinyl-coenzyme A (CoA) and acetyl-CoA.

However, not all observations could be explained based on this catabolic strategy. Evidence has been accumulating that the β-proteobacterium *Azoarcus evansii*, as well as other bacteria, employs an unprecedented strategy to utilize benzoate. The new pathway comprises a number of novel enzymes encoded by specifically induced gene clusters (Fig. 1B) (15). One of the essential features of the new metabolic route is the fact that all intermediates are processed as CoA thioesters (26, 41). Furthermore, after hydroxylation of the aromatic ring, the nonaromatic dihydrodiol intermediate does not rearomatize, as is the case in the usual pathways employing dioxygenases for the introduction of hydroxyl functions. Instead, the ring is directly subjected to oxygen-independent fission. The outlines of the conventional benzoate catabolic pathways and of the unorthodox benzoyl-CoA pathway are summarized in Fig. 1A.

* Corresponding author. Mailing address: Mikrobiologie, Institut Biologie II, Schänzlestr. 1, D-79104 Freiburg, Germany. Phone: (49) 761-2032649. Fax: (49) 761-2032626. E-mail: georg.fuchs@biologie.uni-freiburg.de.

The new pathway is initiated by activation of benzoate to benzoyl-CoA. This reaction is catalyzed by a specifically expressed benzoate-CoA ligase (AMP forming) (26, 41). During the subsequent reaction, benzoyl-CoA is hydroxylated and reduced at positions 2 and 3. The reaction is catalyzed by benzoyl-CoA oxygenase-reductase (40). It is composed of two proteins: an iron-sulfur-flavoprotein reductase (BoxA; 92 kDa) and an oxygenase (BoxB; 55 kDa) (where Box stands for benzoyl-CoA oxidation). These enzymes catalyze the reaction benzoyl-CoA + NADPH + H^+ + O_2 → 2,3-dihydro-2,3-dihydroxybenzoyl-CoA (dihydrodiol) + $NADP^+$.

The dihydrodiol is the substrate for ring fission catalyzed by dihydrodiol lyase BoxC (14). This homodimeric 122-kDa enzyme does not require oxygen and catalyzes the following reaction: 2,3-dihydro-2,3-dihydroxybenzoyl-CoA + H_2O → 3,4-dehydroadipyl-CoA semialdehyde + HCOOH. It is noteworthy that not only benzoate but also phenylacetate (11, 13, 25, 27) and 2-aminobenzoate (4, 18, 33, 35) were shown in various bacteria to be metabolized via unprecedented CoA-dependent new pathways.

In this work, two questions were addressed. First, how is the ring cleavage product 3,4-dehydroadipyl-CoA semialdehyde further metabolized to lead to β-ketoadipate? Second, which enzyme catalyzes the transformation of the semialdehyde to the following intermediate? To produce β-ketoadipate from the semialdehyde, one can envisage its oxidation to the corresponding carboxylic acid at some point.

The benzoate oxidation gene cluster contains an open reading frame (*orf9*) which is located near *boxC* (*orf11*) (Fig. 1B). The product of *orf9* shows similarity to proteins assumed to

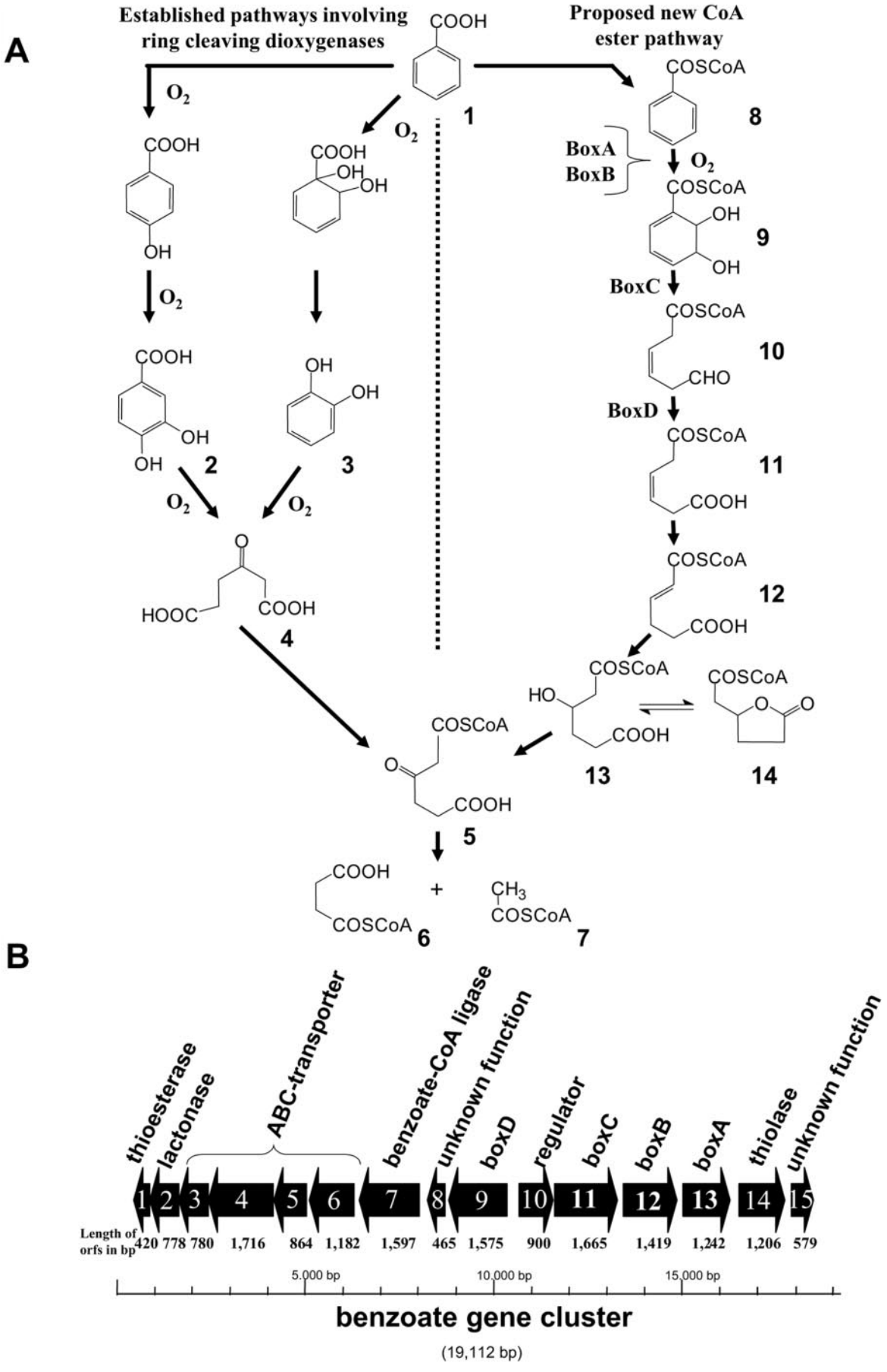
A
Established pathways involving ring cleaving dioxygenases
Proposed new CoA ester pathway
COOH
1
O2
COSCoA
8
BoxA
BoxB
9
BoxC
10
CHO
BoxD
11
12
2
3
4
HOOC
13
14
HO
5
6
7
CH3
B
thioesterase
lactonase
ABC-transporter
benzoate-CoA ligase
unknown function
boxD
regulator
boxC
boxB
boxA
thiolase
unknown function
1 2 3 4 5 6 7 8 9 10 11 12 13 14 15
Length of orfs in bp
420 778 780 1,716 864 1,182 1,597 465 1,575 900 1,665 1,419 1,242 1,206 579
5,000 bp
10,000 bp
15,000 bp
benzoate gene cluster
(19,112 bp)

participate in the aerobic metabolism of phenylacetate in *Escherichia coli* (PaaZ), *A. evansii* (PaaZ), *Pseudomonas putida* (Phal), and presumably other bacteria (12, 15, 26, 28, 30). The amino acid sequence of the *orf9* product shows similarity to aldehyde dehydrogenases (ALDHs). We show that this *orf9* gene product indeed catalyzes the $NADP^+$-dependent oxidation of the ring cleavage product 3,4-dehydroadipyl-CoA semialdehyde to the corresponding acid.

MATERIALS AND METHODS

Materials. Chemicals were obtained from Sigma-Aldrich (Deisenhofen, Germany), Merck (Darmstadt, Germany), and Roth (Karlsruhe, Germany); biochemicals were from Roche Diagnostics (Mannheim, Germany) and Gerbu (Craiberg, Germany). [ring-^{14}C]benzoate was obtained from Amersham Biosciences (Freiburg, Germany), and [ring-$^{13}C_6$]benzoate was purchased from MSD Isotopes (Montreal, Canada). High-pressure liquid chromatography (HPLC) equipment was from Waters (Eschborn, Germany), Phenomenex (Aschaffenburg, Germany), Wicom (Heppenheim, Germany), and Raytest (Straubenhardt, Germany). Enzymes were purchased from MBI Fermentas (St.Leon-Rot, Germany).

Microorganisms and plasmids. *A. evansii* KB740 (DSMZ 6869) (formerly designated *Pseudomonas sp*. KB 740) (2) has been deposited in Deutsche Sammlung für Mikroorganismen und Zellkulturen (Braunschweig, Germany). A mutant of *A. evansii* (*A. evansii*$_{Bhis}$) that contains a His-tagged copy of BoxB (40) was used for purification of enzymes needed for this study. The *E. coli* strain SURE, with the genotype *e14*$^-$ (*mcrA*) Δ(*mcrCB-hsdSMR-mrr*)*171 endA1 supE44 thi-1 gyrA96 relA1 lac recB recJ sbcC umuC*::Tn5 (Kan^r) *uvrC* [F′ *proAB lacI*^{q}*Z* Δ(*M15* Tn*10*) (Tet^r)] from Stratagene (Heidelberg, Germany) and the vector pMal-c2x (NEB, Frankfurt, Germany) were used for overexpression of BoxC and BoxD (14).

Bacterial cultures. Cultivation of *A. evansii*$_{Bhis}$ for the expression and purification of $BoxB_{his}$ was performed as described previously (40). The fusion protein $BoxC_{mal}$ was purified from *E. coli* SURE harboring the recombinant plasmid pMal-c2x/BoxC and grown as previously described (14). For the overexpression of the recombinant protein $BoxD_{mal}$, the *E. coli* SURE cells harboring the plasmid pMal-c2x/BoxD were grown in LB broth containing ampicillin (100 μg/ml) and 11 mM glucose. The cultures were incubated at 37°C with shaking until an optical density at 600 nm of 0.6 was reached; 0.3 mM isopropyl-β-D-thiogalactopyranoside (IPTG) was then added to induce the expression of the fusion protein. After induction, cells were further incubated at 22°C for 4 h and eventually harvested by centrifugation at 8,000 rpm for 10 min. Approximately 75% of the overexpressed $BoxD_{mal}$ fusion protein was soluble.

Preparation of cell extracts. All steps were performed at 4°C. Frozen cells were suspended in an equal volume of 20% glycerol (wt/vol) containing 0.1 mg of DNase I per ml. The suspension was passed through a French pressure cell at 137 MPa and then centrifuged (100,000 × *g*).

Synthesis of coenzyme A thioesters. Benzoyl-CoA was prepared according to previously published procedures (17, 32) with a yield of 65%. [ring-^{14}C]benzoyl-CoA was prepared as published by Zaar et al. (41). The yield was 95%. [ring-$^{13}C_6$]benzoyl-CoA was synthesized as previously described (41). [ring-^{14}C]2,3-dihydro-2,3-dihydroxybenzoyl-CoA (termed dihydrodiol; 66.6 MBq mmol^{-1}) was enzymatically synthesized using purified BoxA and $BoxB_{his}$. A reaction mixture containing 250 ml of 5 mM Tris-HCl (pH 8), 0.2 mM [ring-^{14}C]benzoyl-CoA (66.6 MBq mmol^{-1}), 0.6 mM NADPH, 3.3 mM $MgCl_2$, 3.3 mM glucose 6-phosphate, 100 U of glucose 6-phosphate dehydrogenase, 3.4 mg of BoxA, and 40 mg of $BoxB_{his}$ was stirred at room temperature for 60 min. The reaction was stopped by the addition of ethanol to a final concentration of 10% (vol/vol). After centrifugation (14,000 × *g*; 10 min), the supernatant was diluted threefold with 20 mM NH_4HCO_3, pH 6.9, and applied to a Grom-Sil 120 ODS-4 HE HPLC column (particle size, 11 μm; 250 by 20 mm; Grom, Herrenberg-Kayh, Germany) which was equilibrated with 20 mM NH_4HCO_3, pH 6.9, containing 2% (vol/vol) methanol. The column was developed at a flow rate of 8 ml min^{-1} with 80 ml of equilibration buffer, followed by 160 ml of a linear gradient of 2 to 80% (vol/vol) methanol in water. The benzoyl-CoA-dihydrodiol eluted at 27 min (UV detection at 260 nm with a BioCat UV-Detector; Applied Biosystems, Darmstadt, Germany). The fraction was collected and lyophilized. The ^{14}C recovery was 30%.

Purification of component A (BoxA) and component B_{his} ($BoxB_{his}$) of benzoyl-CoA oxygenase. BoxA was assayed and purified according to Mohamed et al. (26). The purified enzyme solution had a concentration of 0.34 mg ml^{-1}. $BoxB_{his}$ was purified according to Zaar et al. (40). The purified enzyme solution had a concentration of 1.6 mg ml^{-1}.

Purification of $BoxC_{mal}$. $BoxC_{mal}$ was purified according to Gescher et al.(14). The purified enzyme solution had a concentration of 1 mg ml^{-1}.

Construction of an N-terminal fusion of the maltose-binding protein and BoxD. Standard protocols were used for DNA cloning, transformation, amplification, and purification (3, 31). The *boxD* gene was amplified from chromosomal DNA using the primers BoxDBamHIfor (CGGGATCCGTGAAGCTG GCCA ATTACGT) and BoxD*Hind*IIIrev (GGGAAGCTTGGAACTGGGTGTT GGG) (inserted restriction sites are underlined). For complete sequence of the box gene cluster see Gescher et al. (GenBank accession number AF548005) (15). The fragment and the vector pMal-c2x (NEB, Frankfurt, Germany) were cut with BamHI and HindIII and ligated.

Purification of BoxD containing an N-terminal maltose-binding protein tag ($BoxD_{mal}$). $BoxD_{mal}$ was purified in one step at 4°C from 510 mg of protein of an *E. coli* cell extract that contained overexpressed $BoxD_{mal}$. A 25-ml amylose resin column (NEB, Frankfurt, Germany) was equilibrated with 20 mM Tris/HCl (pH 7.4) containing 200 mM NaCl at a flow rate of 1 ml min^{-1}. The column was loaded with extract and washed with 120 ml of the equilibration buffer, followed by elution with 50 ml of the equilibration buffer containing 20 mM of maltose (elution buffer). $BoxD_{mal}$ (9.6 mg) was eluted in 6 ml of the elution buffer. The protein was stored at −20°C in the presence of 10% glycerol.

Gel permeation chromatography. The native molecular mass of $BoxD_{mal}$ was determined by gel permeation chromatography using a 320-ml Superdex 200, Hiload 26/60 column (Amersham Biosciences). The protein sample (5 ml) from the previous chromatographic step was applied to the column, which was equilibrated with 3 bed volumes of the equilibration buffer (10 mM Tris/HCl [pH 8] containing 100 mM KCl). Protein elution was monitored at A_{280}, and fractions of 10 ml (each) were collected and tested for activity. For molecular mass calculations, the column was calibrated with protein molecular mass standards comprising thyroglobulin (660 kDa), ferritin (440 kDa), catalase (220 kDa), aldolase (160 kDa), bovin serum albumin (67 kDa), ovalbumin (45 kDa), dextran blue (2,000 kDa), and vitamin B_{12} (1.3 kDa).

Assays for $BoxD_{mal}$ activity. (i) Photometric assay. Two assays were used. For the photometric assay, microtiter plate assay mixtures (200 μl) contained 100 mM morpholinepropanesulfonic acid (MOPS; pH 7.2), 30 μl of $BoxC_{mal}$ (30 μg), 15 μl of diluted $BoxD_{mal}$ (1.2 μg of protein), 4 mM NADP, and 0.2 mM dihydrodiol (66.6 MBq mmol^{-1}). The dihydrodiol was first converted to 3,4-dehydroadipyl-CoA semialdehyde by $BoxC_{mal}$. This reaction was followed at 310 nm (14) (μQuant Universal Microplate spectrophotometer; BIO-TEK Instruments, Bad Friedrichshall, Germany) ($\varepsilon_{310} = 7 \times 10^3$ M^{-1} cm^{-1}). After complete conversion of the dihydrodiol to the semialdehyde, the reaction catalyzed by $BoxD_{mal}$ was started by the addition of $NADP^+$. $NADP^+$ reduction was followed spectrophotometrically at 365 nm (μQuant Universal Microplate spectrophotometer; BIO-TEK Instruments, Bad Friedrichshall, Germany) ($\varepsilon_{365\ nm}$ (NADH) = 3.4 10^3 M^{-1} cm^{-1}). The amount of BoxD with an N-terminal maltose-binding protein tag ($BoxD_{mal}$) was varied from 0 to 4 μg when the protein dependence of the reaction was studied. $BoxD_{mal}$ was also used to determine the V_{max}, the apparent K_m values, and the pH optimum. $BoxD_{mal}$ activity was tested at different pH values in three different buffers (morpholineethanesulfonic acid [MES], pH 6 to 6.7; MOPS, pH 6.7 to 7.9; and Tricine, pH 7.9 to 8.8).

HPLC assays. Assays and intermediate analysis were performed according to Zaar et al. (41) with slight modifications. The standard assay mixture (0.25 ml;

FIG. 1. (A) The proposed new aerobic benzoate metabolic pathway in *A. evansii* and the conventional β-ketoadipate pathway. Compounds: 1, benzoate; 2, protocatechuate; 3, catechol; 4, β-ketoadipate; 5, β-ketoadipyl-CoA; 6, succinyl-CoA; 7, acetyl-CoA; 8, benzoyl-CoA; 9, 2,3-dihydro-2,3-dihydroxybenzoyl-CoA; 10, 3,4-dehydroadipyl-CoA semialdehyde; 11, *cis*-3,4-dehyroadipyl-CoA; 12, *trans*-2,3-dehydroadipyl-CoA; 13, β-hydroxyadipyl-CoA; 14, β-hydroxyadipyl-CoA lactone. The two pathways merge at β-ketoadipyl-CoA (compound 5). (B) The aerobic benzoate oxidation gene cluster of *A. evansii* is experimentally shown, as well as putative functions of the gene products. The sizes of the different open reading frames are indicated beneath the arrows.

22°C) contained 0.6 mM NADPH, 0.2 mM [ring-^{14}C]benzoyl-CoA (66.6 MBq mmol^{-1}), 3.4 μg BoxA, 100 μg BoxB, 10 μg $BoxC_{mal}$, and 10 μg $BoxD_{mal}$. For the separation of intermediates formed from [ring-^{14}C]benzoyl-CoA, samples were applied to a column of ReproSil C18-Column (particle size, 5 μm; 125 by 4 mm; flow rate, 1 ml min^{-1}) (41). Retention times were as follows: polar products, 1.5 min; benzoate, 6 min; *cis*-3,4-dehydroadipyl-CoA, 22 min; 3,4-dehydroadipyl-CoA semialdehyde, 33.5 min; *cis*-2,3-dihydro-2,3-dihydroxybenzoyl-CoA, 35 min; and benzoyl-CoA, 41 min.

UV-visible spectroscopy. Absorption spectra of purified $BoxD_{mal}$ (1.6 mg ml^{-1}) were determined as described for BoxA (26). Enzymes obtained from affinity chromatography were considered oxidized.

Sodium dodecyl sulfate-polyacrylamide gel electrophoresis of protein and protein determination. Polyacrylamide (10%) gel electrophoresis was performed according to the Laemmli method (9). Proteins were visualized by Coomassie blue staining (42). Molecular mass standards were phosphorylase b, bovine serum albumin, ovalbumin, lactate dehydrogenase, carbonic anhydrase, and lysozyme (97, 67, 45, 34, 29, and 14 kDa, respectively). Protein was determined by Bradford method (9) using bovine serum albumin as a standard.

Large-scale conversion of [ring-$^{13}C_6$]benzoyl-CoA with purified BoxA, $BoxB_{his}$, $BoxC_{mal}$, and $BoxD_{mal}$. To 50 ml of 5 mM Tris-HCl (pH 8) containing 12 mg of [ring-^{13}C]benzoyl-CoA (0.27 mM), 0.6 mM NADPH, 5 mg of BoxA, 20 mg of $BoxB_{his}$, 5 mg of $BoxC_{mal}$, and 5 mg $BoxD_{mal}$ were added. The reaction mixture was stirred at room temperature for 60 min and then acidified to pH 5 by addition of 500 μl of 1% (vol/vol) formic acid. [ring-^{13}C]Benzoyl-CoA was completely consumed. After centrifugation (14,000 × *g*; 10 min), the supernatant was applied to four strataX (Phenomenex) solid-phase extraction columns (500-mg phase; 12-ml reservoir volume), which had been equilibrated with 20 mM NH_4HCO_3, pH 5, containing 1% (vol/vol) ethanol. The columns were washed with 1 reservoir volume of equilibration buffer. The product which bound to the material was eluted with 100% (vol/vol) methanol. The fractions were pooled and reduced to 1 ml by flash evaporation at 30°C and 4 kPa, 500 μl was lyophilized, and the remaining 500 μl was kept frozen at −70°C. The frozen sample was analyzed by nuclear magnetic resonance (NMR) spectroscopy, although lyophilization did not lead to decay products of the purified intermediate.

NMR spectroscopy. A total of 50 μl of D_2O was added to the reaction mixtures. ^{1}H and ^{13}C NMR spectra were measured at 20°C with a Bruker DRX 500 spectrometer with a ^{13}C ^{1}H dual probe head. The chemical shifts were referenced to external tetramethylsilane.

Mass spectroscopy. Mass spectroscopy was conducted by the electrospray-ionization procedure in negative ion mode, using Thermo Finnigan LCQ Advantage apparatus (capillary temperature, 330°C; source-induced dissociation voltage, 10 V; Thermo Electron, Dreieich, Germany).The instrument was coupled to a Surveyor HPLC system with a Reprosil C_{18} column (particle size, 5 μm; 4 by 125 mm; Wicom, Heppenheim, Germany). HPLC separations were conducted using an acetonitrile gradient from 2% (vol/vol) to 10% (vol/vol) itriethylammoniumcarbonate (1 M) over a period of 25 min with a flow rate of 0.5 ml/min. The mass spectrum was recorded in the region *m/z* 250 to 1,200.

RESULTS

3,4-Dehydroadipyl-CoA semialdehyde-transforming activity in cell extracts of *A. evansii*. Unlabeled and [^{14}C]-labeled 3,4-dehydroadipyl-CoA semialdehyde was enzymatically prepared from benzoyl-CoA using benzoyl-CoA oxygenase-reductase (BoxBA) and the recombinant ring-cleaving dihydrodiol lyase $BoxC_{mal}$. Transformation of the 3,4-dehydroadipyl-CoA semialdehyde was studied in cell extracts by a continuous spectrophotometric assay based on the reduction of $NADP^+$. Extracts of cells grown aerobically on benzoate catalyzed the 3,4-dehydroadipyl-CoA semialdehyde-dependent reduction of $NADP^+$ with a specific activity of 0.17 μmol min^{-1} mg^{-1} cell protein. HPLC analysis revealed complete transformation of the substrate to new products. Almost no product formation was observed with NAD^+. The 3,4-dehydroadipyl-CoA semialdehyde-transforming enzyme was contained in the soluble cell fraction and was strictly regulated. Activity in cells grown anaerobically on benzoate and nitrate (0.010 μmol min^{-1} mg^{-1} cell protein) or grown aerobically on acetate (0.014 μmol min^{-1} mg^{-1} cell protein) was 1 order of magnitude lower, indicating regulation, probably on the transcriptional level. Interestingly, cells grown aerobically on phenylacetate showed a relatively high activity of 0.045 μmol min^{-1} mg^{-1} cell protein.

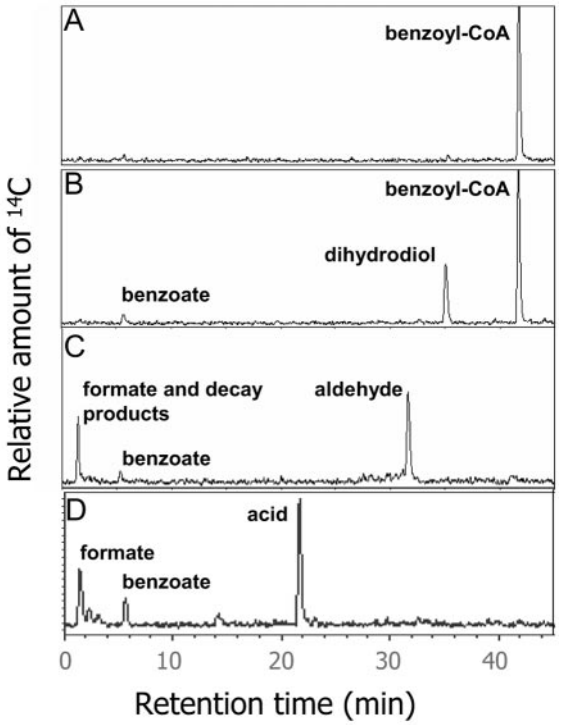

FIG. 2. HPLC separations of [ring-$^{14}C_6$]-benzoyl-CoA and products resulting from its conversion with purified Box enzymes. Benzoyl-CoA (A), 2,3-dihydro-2,3-dihydroxybenzoyl-CoA (dihydrodiol) resulting from transformation of benzoyl-CoA with the oxygenase/reductase (BoxBA) (B), and 3,4-dehydroadipyl-CoA semialdehyde and formate (C) are the products resulting from the hydrolytic ring opening of the dihydrodiol as catalyzed by $BoxC_{mal}$. (D) Transformation of the semialdehyde to the corresponding acid 3,4-dehydroadipyl-CoA is catalyzed by $BoxD_{mal}$. The small amount of benzoate results from the thioesterase action on benzoyl-CoA.

Construction of an *orf9* clone encoding an N-terminal maltose-binding protein fusion protein, expression in *E. coli*, and purification and characterization of the protein. A postulated putative long-chain aldehyde dehydrogenase gene (*orf9*), which might encode the 3,4-dehydroadipyl-CoA semialdehyde-oxidizing enzyme BoxD, is located on a cluster of genes encoding enzymes and a transport system required for aerobic benzoate oxidation in *A. evansii* (see the introduction) (Fig. 1B). The gene encodes a 54-kDa protein, which has similarity to MaoC protein (13). This gene was cloned and successfully expressed in *E. coli* as a protein tagged at its N terminus with maltose-binding protein. The expected monomer size of the recombinant protein was 96 kDa. Such a protein was obtained with a high yield by chromatography on amylose resin and maltose for elution. The recombinant protein catalyzed the 3,4-dehydroadipyl-CoA semialdehyde-dependent reduction of $NADP^+$ and is referred to as $BoxD_{mal}$, 3,4-dehydroadipyl-CoA semialdehyde dehydrogenase ($NADP^+$). The affinity chromatography resulted in a 47-fold enrichment of the activity.

Product formation from ^{14}C-labeled benzoyl-CoA was fol-

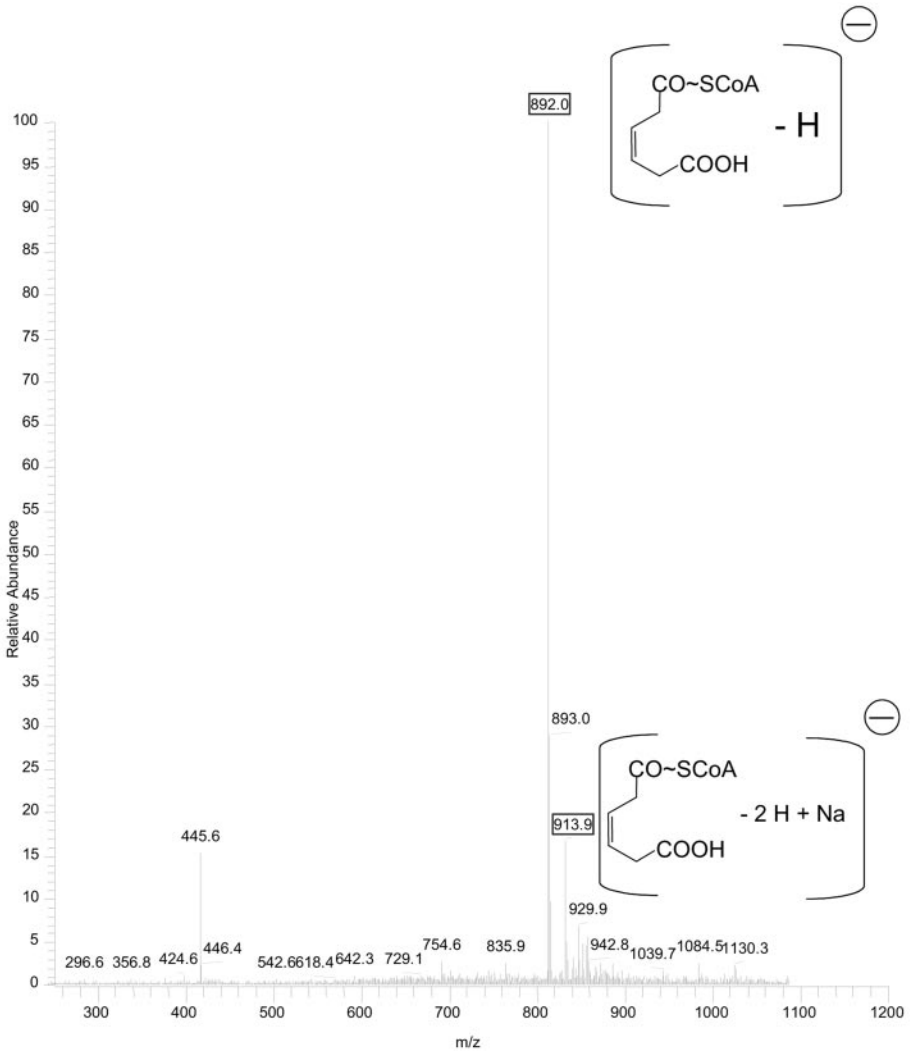

FIG. 3. Mass spectroscopic analysis of the new intermediate arising from the conversion of the ring cleavage product 3,4-dehydroadipyl-CoA semialdehyde with $BoxD_{mal}$. The spectrum shows a main peak at 892 Da that agrees well with the theoretical mass of the corresponding acid (see Discussion).

lowed by HPLC (Fig. 2). When BoxA and BoxB alone were added in the presence of NADPH, benzoyl-CoA was incompletely converted to its dihydrodiol. Addition of BoxC to this assay resulted in complete conversion to the ring fission product semialdehyde and formate. When BoxD was also included, the semialdehyde was completely consumed and converted to a new product. This product had a UV absorption similar to that of coenzyme A, with an absorption maximum at 259 nm. In all experiments, traces of benzoate were formed by hydrolysis of benzoyl-CoA. The enzyme eluted in two distinct peaks during gel filtration chromatography. Part of the enzyme (25%) eluted at a molecular mass of around 2,500 kDa, indicating that a large oligomer was formed; however, the majority (75%) eluted at a molecular mass of 180 kDa, most probably in form of a homodimer. The formation of large oligomers is well known for members of the aldehyde dehydrogenase enzyme family (22). The specific activity corrected for the size of the untagged protein was 7.5 μmol min^{-1} mg^{-1} protein. In comparing the specific activity of the purified recombinant enzyme with that of the extract of benzoate-induced cells (0.17 μmol min^{-1} mg^{-1} protein), it follows that this enzyme constitutes approximately 0.2% of the soluble cell protein. Since the recombinant protein was highly active, it was used in the following studies.

Characterization of 3,4-dehydroadipyl-CoA semialdehyde dehydrogenase ($NADP^+$). The UV-visible spectrum of the oxidized, colorless $BoxD_{mal}$ protein (not shown) shows an absorption maximum at 280 nm, which is due to protein absorption. The molar absorption coefficient at 280 nm of 103,000 M^{-1} cm^{-1} compared well with the theoretical value of 99,000 M^{-1} cm^{-1}, based on the deduced amino acid sequence. The enzyme could be stored without appreciable loss of activity for months at −20°C in the presence of 10% (vol/vol) glycerol.

The kinetics were studied by a spectrophotometric assay in which the semialdehyde-dependent reduction of $NADP^+$ was followed. The tagged enzyme had a V_{max} of 7.5 ± 0.5 μmol min^{-1} mg^{-1} (corrected for the size of the untagged enzyme), a K_m for the 3,4-dehydroadipyl-CoA semialdehyde of 25 ± 3

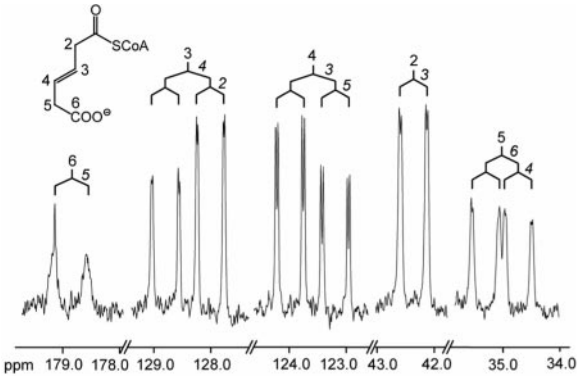

FIG. 4. ^{13}C NMR signals of [2,3,4,5,6-$^{13}C_5$]3,4-dehydroadipyl-CoA (top) obtained from a reaction mixture containing [ring-^{13}C]benzoyl-CoA, NADPH, and BoxABCD. The spectrum was recorded after protein precipitation, solid-phase extraction, and concentration of the eluent. The coupling pattern is indicated.

μM, and a K_m for $NADP^+$ of 16 μM ± 4 μM. The turnover number corrected for the size of a dimer of the untagged enzyme was 45 s^{-1} and k_{cat}/K_m was calculated to 1,800,000 s^{-1} M^{-1}. The enzyme had a pH optimum of 7.2 and showed half-maximal activity at pH 6.2 and 8.8. Salt concentrations up to 500 mM KCl and EDTA concentrations up to 50 mM had no effect on enzyme activity. The molar ratio of moles of converted substrate per moles of NADPH formed was estimated to be 1. $BoxD_{mal}$ showed no activity (<2%) when NAD^+ was used instead of $NADP^+$.

Structural analysis of the reaction product by mass spectroscopy. The mass spectrum revealed a molecular mass of 892 Da (Fig. 3). The latter could be attributed to the acid 3,4-dehydroadipyl-CoA or the corresponding β-hydroxyadipyl-CoA lactone. Moreover, the mass spectrum showed an additional mass at 914 Da, due to binding of a sodium ion to the CoA.

Structure elucidation of the reaction product by NMR spectroscopy. The recombinant $BoxD_{mal}$ protein was incubated aerobically at 22°C with 12 mg of [ring-$^{13}C_6$]benzoyl-CoA in the presence of BoxA, BoxB, and $BoxC_{mal}$ protein and 0.6 mM $NADP^+$. After 60 min, the sample was deproteinized by the addition of formic acid. The sample was centrifuged, and the supernatant was subjected to NMR analysis after solid-phase extraction and concentration. Due to the ^{13}C enrichment of the substrate, only signals arising from the ^{13}C-labeled ring carbon atoms were selectively detected in the ^{13}C NMR spectrum of the crude reaction mixture. Indeed, only five intense ^{13}C-coupled ^{13}C NMR signals (Fig. 4; Table 1) were observed. The doublet structure of the signals at 178.8 and 42.3 ppm signaled that each these signals was caused from a carbon atom connected to only one adjacent ^{13}C atom. Three signals were double doublets, reflecting that each of the respective atoms had two ^{13}C-labeled neighbors. The smaller signal splittings (2 to 4 Hz) were due to long-range couplings via two or three bonds. The chemical shifts indicated the presence of a carboxylic acid function (doublet at 178.8 ppm), a carbon-carbon double bond (double doublets at 128.4 and 123.5 ppm, respectively), and two methylene carbon atoms (doublet at 42.3 and double doublet at 35.0 ppm, respectively). The connectivity of these atoms was determined by the detailed analysis of the ^{13}C-^{13}C coupling pattern. On the basis of the coupling constant of 52.8 Hz observed for each of the signals at 178.8 ppm (reflecting the carboxylic acid atom C-6) (Figure 5); at 35.0 ppm, the carboxylic acid atom was connected to the methylene carbon atom C-5. The latter atom gave rise to a second ^{13}C coupling with a coupling constant of 42.3 Hz, which is also detected for the signal at 123.5 ppm. On this basis, the signal at 123.5 ppm has to be assigned as C-4, establishing one carbon atom of the double bond. As expected, the signal at 123.5 ppm also showed a coupling constant of 71.5 Hz, which is typical for a coupling between ^{13}C atoms of a double bond. The second atom of the double bond (C-3) resonated at 128.4 ppm and showed couplings of 72.0 and 42.0 Hz. The smaller coupling constant was also seen for the doublet at 42.3 ppm, which therefore has to be assigned as C-2. The chemical shift of C-2 is typical for a methylene carbon atom connected to a thioester moiety. The corresponding thioester carbon atom was not observed in the ^{13}C NMR spectrum, since it is not ^{13}C enriched from the labeled [ring-$^{13}C_6$]benzoyl-CoA. However, the ^1H NMR spectrum of the compound showed the expected signals for a coenzyme A residue. Therefore, the structure of the compound is assigned as [2,3,4,5,6-$^{13}C_5$]3,4-dehydroadipyl-CoA. It should be noted that the transformation of benzoyl-CoA (C-7 compound) into 3,4-dehydroadipyl-CoA (C-6 compound) implicates the loss of one carbon atom as $H^{13}COOH$ (14).

DISCUSSION

General properties and role of the enzyme. BoxD represents a new aldehyde dehydrogenase acting on 3,4-dehydroadipyl-CoA and using $NADP^+$ as an electron acceptor (EC 1.2.1.x). The following features are in line with the suggested role of the enzyme in the benzoyl-CoA catabolic pathway: (i) its regulation (up-regulation under aerobic conditions in the presence of benzoate); (ii) the position of the *boxD* gene in the part of the gene cluster also encoding the first enzyme in the pathway, benzoate-CoA ligase; (iii) the specific activity of the enzyme in cell extract, which is sufficient to explain aerobic growth with benzoate; and (iv) the low apparent K_m values for its aldehyde substrate and cosubstrate $NADP^+$. The lower "induction" by phenylacetate may be gratuitous and be caused by the structural similarity of the putative derepressor benzoate (or benzoyl-CoA) with phenylacetate (or phenylacetyl-CoA) (3a). Alternatively, a similar promiscuous dehydrogenase may be involved in aerobic phenylacetate metabolism that also acts on 3,4-dehydroadipyl-CoA semialdehyde. The $NADP^+$ specificity of the dehydrogenase fits nicely with the NADPH specificity of the benzoyl-CoA oxygenase-reductase, thus forming a small $NADP^+$-dependent cycling of reducing equivalents.

The enzyme is the fifth enzyme in the unorthodox benzoyl-

TABLE 1. ^{13}C-NMR data of [2,3,4,5,6-$^{13}C_5$]3,4-dehydroadipyl-CoA

Position	Chemical shift (ppm) of $\delta^{13}C$	Coupling constant (Hz) of J_{cc}
6	178.8 (d)	52.8
3	128.4 (dd)	72.0, 41.5, 2.5
4	123.5 (dd)	71.5, 42.3, 4.0
2	42.3 (d)	42.3, 4.0
5	35.0 (dd)	52.8, 42.3, 2.6

FIG. 5. Partial alignment of the ALDH2 protein sequence, of the aldehyde dehydrogenases from *S. mutans* and *V. harveyi*, and of BoxD from *A. evansii*. Conserved amino acids which function in cofactor binding and specificity are highlighted by letters in boldface type, the catalytic cysteine residue is highlighted in black, the two conserved glutamate residues that might function in the activation of the cysteine nucleophile are highlighted in gray, and the histidine residue that is involved in the catalytic mechanism of the *V. harveyi* enzyme and eventually BoxD is highlighted by a capital letter.

CoA catabolic pathway (see the introduction) (Fig. 1A). The enzymes and intermediates in the conversion of 3,4-dehydroadipyl-CoA, presumably to 3-oxoadipyl-CoA, are not yet known. 3-Oxoadipyl-CoA, an intermediate which is common in the classical 3-oxoadipate pathway, is most likely thiolytically cleaved to acetyl-CoA and succinyl-CoA by β-ketothiolase, and the corresponding putative gene (*orf11*) is carried in that part of the benzoate oxidation gene cluster which also encodes the oxygenase-reductase BoxBA and the ring-opening enzyme BoxC (Fig. 1B). 3,4-Dehydroadipyl-CoA may form a lactone ring (β-hydroxyadipyl-CoA lactone), which may be the substrate of the lactonase encoded by *orf2* (15). β-Hydroxyadipyl-CoA lactone is one of the additional intermediates, which were found by NMR analysis of intermediates occurring after conversion of benzoyl-CoA with *A. evansii* crude extracts (41). A putative thioesterase, whose gene (*orf1*) is adjacent to the putative lactonase gene *orf2*, may function as a security valve by hydrolyzing CoA thioester intermediates in case of a metabolic block, thus preventing the deprivation of CoA and cell death by metabolic collapse (15).

Identity of the reaction product. Conversion of the ring cleavage product, 3,4-dehydroadipyl-CoA semialdehyde, with the purified $BoxD_{mal}$ gave a new intermediate. Analysis of the latter by mass spectroscopy revealed a main molecular mass of 892 Da. This could be attributed to two different compounds. The first candidate is 3,4-dehydroadipyl-CoA. The alternative is β-hydroxyadipyl-CoA lactone. Both compounds were found during the transformation of benzoyl-CoA with a cell extract of *A. evansii*, where they had obviously different elution times upon HPLC analysis (41). Therefore, it is not possible to assign the observed mass to either of the compounds, based only on the results of the mass spectra. To disclose the structure of the reaction product, the product was prepared in a large-scale conversion of [ring-$^{13}C_6$]benzoyl-CoA with purified Box enzymes (BoxA, $BoxB_{His}$, $BoxC_{mal}$, and $BoxD_{mal}$) and analyzed by NMR-spectroscopy. The NMR data revealed unambiguously that the new intermediate was 3,4-dehydroadipyl-CoA. However, it cannot be excluded that the lactone originates from the acid and then undergoes interconversion with β-hydroxyadipyl-CoA. This could then yield β-ketoadipyl-CoA via dehydrogenation (Fig. 1A).

Similar genes of BoxD in the database. BoxD is part of the Box gene cluster of *A. evansii* that contains at least 15 genes altogether (accession number AF548005) (15). Genome sequencing projects revealed that similar gene clusters are present in *Azoarcus evansii* strain EbN1, *Burkholderia xenovorans* (formerly *Burkholderia fungorum*) (16), *Ralstonia metallidurans*, *Magnetospirillum magnetotacticum*, *Rhodopseudomonas palustris*, *Silicibacter pomeroyi*, *Bradyrhizobium japonicum*, *Polaromonas* sp., and *Ralstonia eutropha*. Interestingly, an ortholog to BoxD can only be found in four out of the nine clusters (*B. xenovorans*, *A. evansii* Ebn1, *Polaromonas* sp., and *M. magnetotacticum*), indicating that in five organisms other aldehyde dehydrogenases will eventually fulfill the role of BoxD in the benzoate degradation pathway. An alignment of BoxD with its four known orthologs reveals sequence similarities (identity) of the deduced amino acid sequences between 65% (52%) and 88% (83%).

Comparison of the BoxD primary sequence to known aldehyde dehydrogenases. BoxD is a member of the large family of ALDHs (EC 1.2.1.3 and 1.2.1.5). ALDHs are $NAD(P)^+$-dependent enzymes that catalyze the oxidation of aldehydes to their corresponding carboxylic acids (30). The reaction proceeds via formation of a covalent thiohemiacetal intermediate through binding of an aldehyde to an enzyme-NAD(P) complex. The thiohemiacetal is subsequently oxidized to a thioacyl intermediate. Deacetylation leads to the corresponding carboxylic acid (39).

The majority of known aldehyde dehydrogenases are NAD^+ dependent. Two families, nonphosphorylating glyceraldehyde 3-phosphate dehydrogenase and 10-formyltetrahydrofolate dehydrogenase, are strictly $NADP^+$ specific. One class of aldehyde dehydrogenases, class 3, can use both cofactors in vitro, showing higher activity with NADP. Several structures of enzymes belonging to the aldehyde dehydrogenase superfamily are available.

An alignment of the protein sequence of BoxD with the NAD^+-specific mitochondrial aldehyde dehydrogenase (ALDH 2; accession number P20000) (34) and with $NADP^+$-specific

aldehyde dehydrogenases from *Vibrio harveyi* (accession number AAA89078) (1) and *Streptococcus mutans* (accession number Q59931) (7, 8) reveals its affiliation to the ALDH superfamily (Fig. 5). The structures of all three enzymes have been solved. BoxD shows an overall similarity to any of the three enzymes of 23% with expected values in an alignment ranging from 1×10^{-5} (for the *V. harveyi* enzyme) to 5×10^{-19} (for the *S. mutans* enzyme). Among the invariant amino acids in all ALDHs is only one cysteine residue (Cys_{302} in ALDH2, Cys_{284} in the *V. harveyi*, and Cys_{289} in *S. mutans* enyzme). This residue most likely forms the thiohemiacetal intermediate with the substrate (12, 21, 37, 38). BoxD shows this cysteine residue at amino acid position 294. Furthermore, two glutamic acid residues are invariant in ALDHs (Glu_{268} and Glu_{399} in ALDH2, Glu_{253} and Glu_{377} in *V. harveyi*, and Glu_{250} and Glu_{377} in *S. mutans*). Depending on the specific ALDH, one or the other of these glutamate residues has been proposed to act as a general base that activates the cysteine nucleophile (20, 38, 43). Homologs to these glutamate residues can be found in BoxD at positions 255 and 399. However, in the structures of the three ALDHs mentioned here, the glutamate residues are at least 5-Å away from the catalytic cysteine residue, meaning that the effect of the glutamate might not be direct but via a water molecule or another polar residue. For the *V. harveyi* enzyme, it was shown that a histidine residue (His_{450}), which is in close proximity to the catalytic cysteine, increases thiohemiacetal-forming activity (43). Although this His residue is not generally conserved in all ALDHs, it can be found beside the Glu residues in BoxD (His_{476}) and in all orthologs of the enzyme. This might indicate that the catalytic mechanism of BoxD is similar to that of the long-chain aliphatic aldehyde dehydrogenase of *V. harveyi*.

ALDHs contain the characteristic Rossman fold of $NAD(P)^+$-binding proteins (24). The fingerprint of this fold is the amino acid sequence GXXXXG. Mutation studies with the *V. harveyi* ALDH have shown that the second glycine residue is not absolutely critical for cofactor binding but that mutation of the first glycine results in decreased NAD^+ and $NADP^+$ binding (36). A homologous first Gly residue (Gly_{231}) can be found in BoxD and in all orthologs of BoxD in the database, while the second Gly residue is missing in BoxD and in its orthologs. Specificity towards either NAD^+ or $NADP^+$ seems to be largely determined by a glutamate residue that in NAD^+-specific ALDHs coordinates the 2′ and 3′ hydroxyls of the adenine ribose of NAD while potentially repelling the 2′ phosphate of $NADP^+$ (Glu_{195} in ALDH2) (29). In the $NADP^+$-specific ALDHs from *V. harveyi* and *S. mutans*, a threonine (Thr_{180} or Thr_{175}) instead of a glutamate residue can be found, which hydrogen bonds with its side chain to the 2′ phosphate of $NADP^+$. A homologous threonine residue can be found in BoxD (Thr_{183}) and in its orthologs, underlining the experimentally determined specificity towards $NADP^+$.

Interestingly, BoxD shows also strong similarity to the PaaZ protein of *E. coli* (40% identical amino acids; expected value, 10^{-104}) and, to a lesser extent, of *A. evansii*; these proteins were proposed to be the ring-cleaving proteins in the aerobic phenylacetic acid degradation pathway (13, 23, 26). The *E. coli* protein contains two domains. The C-terminal domain is an enoyl-CoA hydratase domain (28), while the N terminus shows strong similarity to BoxD and other members of the ALDH protein family. Since the aerobic pathways of benzoate degradation in *A. evansii* and of phenylacetate degradation in *E. coli* and *A. evansii* show strong similarities (14), it is reasonable to propose that the ALDH domain of PaaZ protein might catalyze a reaction and a substrate similar to those of BoxD. This could explain the high levels of activity in a BoxD enzyme assay of extracts from cells that were aerobically grown on phenylacetic acid.

ACKNOWLEDGMENTS

This work was supported by the Deutsche Forschungsgemeinschaft, by Land Baden-Württemberg (Landesgraduiertenstipendium), and by Fonds der Chemischen Industrie.

Thanks to Nasser Gad'on and Christa Ebenau-Jehle for expert technical assistance and to Christoph Warth, Organische Chemistry, Universität Freiburg, for mass spectrometry.

REFERENCES

1. **Ahvazi, B., R. Coulombe, M. Delarge, M. Vedadi, L. Zhang, E. Meighen, and A. Vrielink.** 2000. Crystal structure of the $NADP^+$-dependent aldehyde dehydrogenase from *Vibrio harveyi*: structural implications for cofactor specificity and affinity. Biochem. J. **349:**853–861.
2. **Anders, J. H., A. Kaetzke, P. Kämpfer, W. Ludwig, and G. Fuchs.** 1995. Taxonomic position of aromatic-degrading denitrifying pseudomonad strains K172 and KB740 and their description as new members of genera *Thauera*, as *Thauera aromatica* sp. nov., and *Azoarcus*, as *Azoarcus evansii* sp. nov., respectively, members of the beta subclass of the *Proteobacteria*. Int. J. Syst. Bacteriol. **45:**327–333.
3. **Ausubel, F. M., R. Brent, R. E. Kingston, D. D. Moore, J. G. Seidman, J. A. Smith, and K. Struhl.** 1987. Current protocols in molecular biology. John Wiley and Sons, New York, N.Y.

3a. **Barragan, M. F., B. Blazquez, M. T. Zamarro, J. M. Mancheno, J. L. Garcia, E. Diaz, and M. Carmona.** 2005. BzdR, a repressor that controls the anaerobic catabolism of benzoate in Azoarcus sp. CIB, is the first member of a new subfamily of transcriptional regulators. J. Biol. Chem. **280:**10683–10694.

4. **Buder, R., and G. Fuchs.** 1989. 2-Aminobenzoyl-CoA monooxygenase/reductase, a novel type of flavoenzyme. Purification and some properties of the enzyme. Eur. J. Biochem. **185:**629–635.
5. **Bugg, T. D. H.** 2003. Dioxygenase enzymes: catalytic mechanisms and models. Tetrahedron **59:**7075–7101.
6. **Butler, C. S. and Mason, J. R.** 1997. Structure-function analysis of the bacterial aromatic ring-hydroxylating dioxygenases. Adv. Microb. Physiol. **38:**47–84.
7. **Cobessi, D., F. Tete-Favier, S. Marchal, G. Branlant, and A. Aubry.** 2000. Structural and biochemical investigations of the catalytic mechanism of an NADP-dependent aldehyde dehydrogenase from *Streptococcus mutans*. J. Mol. Biol. **300:**141–152.
8. **Cobessi, D., F. Tete-Favier, S. Marchal, S. Azza, G. Branlant, and A. Aubry.** 1999. Apo and holo crystal structures of an NADP-dependent aldehyde dehydrogenase from *Streptococcus mutans*. J. Mol. Biol. **290:**161–173.
9. **Coligan, J. E., B. M. Dunn, H. L. Ploegh, D. W. Speicher, and P. T. Wingfield.** 1995. Current protocols in protein science. John Wiley & Sons, New York, N.Y.
10. **Dagley, S.** 1978. Pathways for the utilization of organic substrates, p 305–388. *In* J. R. Sokatch and L. N. Ornston (ed.), The bacteria. Academic Press, New York, N.Y.
11. **Diaz, E., A. Ferrandez, M. A. Prieto, and J. L. Garcia.** 2001. Biodegradation of aromatic compounds by *Escherichia coli*. Microbiol. Mol. Biol. Rev. **65:** 523–568.
12. **Farres, J., T. T. Wang, S. J. Cunningham, and H. Weiner.** 1995. Investigation of the active site cysteine residue of rat liver mitochondrial aldehyde dehydrogenase by site-directed mutagenesis. Biochemistry **34:**2592–2598.
13. **Ferrandez, A., B. Minamberes, B. Garcia, E. R. Olivera, J. M. Luengo, J. L. Garcia, and E. Diaz.** 1998. Catabolism of phenylacetic acid in *Escherichia coli*. J. Biol. Chem. **273:**25974–25986.
14. **Gescher, J., W. Eisenreich, J. Wörth, A. Bacher, and G. Fuchs.** 2005. Aerobic benzoyl-CoA catabolic pathway in *Azoarcus evansii*: studies on the non-oxygenolytic ring cleavage enzyme. Molecular Microbiology **56:**1586–1600.
15. **Gescher, J., A. Zaar, M. Mohamed, H. Schägger, and G. Fuchs.** 2002. Genes coding for a new pathway of aerobic benzoate metabolism in *Azoarcus evansii*. J. Bacteriol. **184:**6301–6315.
16. **Goris, J., P. De Vos, J. Caballero-Mellado, J. Park, E. Falsen, J. F. 3rd Quensen, V. M. Tiedje, and P. Vandamme.** 2004. Classification of the biphenyl- and polychlorinated biphenyl-degrading strain LB400T and relatives as *Burkholderia xenovorans* sp. nov. Int. J. Syst. Evol. Microbiol. **54:**1677–1681.
17. **Gross, G. G., and M. H. Zenk.** 1966. Darstellung und Eigenschaften von Coenzym A-Thioestern substituierter Zimtsäuren. Z. Naturforsch. B **21:**683–690.

18. **Hartman, S., C. Hultschig, W. Eisenreich, G. Fuchs, A. Bacher, and S. Ghisla.** 1999. NIH shift in flavine dependent monooxygenation: mechanistic studies with 2-aminobenzoyl-CoA monooxygenase/reductase. Proc. Natl. Acad. Sci. USA **96:**7831–7836.
19. **Harwood, C. S., and Parales, R. E.** 1996. The beta- ketoadipate pathway and the biology of self-identity. Annu. Rev. Microbiol. **50:**553–590.
20. **Hempel, J., J. Perozich, T. Chapman, J. Rose, J. S. Boesch, Z. J. Liu, R. Lindahl, and B. C. Wang.** 1999. Aldehyde dehydrogenase catalytic mechanism. A proposal. Adv. Exp. Med. Biol. **463:**53–59.
21. **Hempel, J., H. Nicholas, and R. Lindahl.** 1993. Aldehyde dehydrogenases: widespread structural and functional diversity within a shared framework. Protein Sci. **2:**1890–1900.
22. **Ichihara, K., Y. Noda, C. Tanaka, and M. Kusunose.** 1986. Purification of aldehyde dehydrogenase reconstitutively active in fatty alcohol oxidation from rabbit intestinal microsomes. Biochim. Biophys. Acta **878:**419–425.
23. **Ismail, W., M. El-Said Mohamed, B. L. Wanner, K. A. Datsenko, W. Eisenreich, F. Rohdich, A. Bacher, and G. Fuchs.** 2003. Functional genomics by NMR spectroscopy. Phenylacetate catabolism in *Escherichia coli*. Eur. J. Biochem. **270:**3047–3054.
24. **Liu, Z. J., Y. J. Sun, J. Rose, Y. J. Chung, C. D. Hsiao, W. R. Chang, I. Kuo, J. Perozich, R. Lindahl, J. Hempel, and B. C. Wang.** 1997. The first structure of an aldehyde dehydrogenase reveals novel interactions between NAD and the Rossmann fold. Nat. Struct. Biol. **4:**317–326.
25. **Mohamed, M. E., W. Ismail, J. Heider, and G. Fuchs.** 2002. Aerobic metabolism of phenylacetic acids in *Azoarcus evansii*. Arch. Microbiol. **178:**180–192.
26. **Mohamed, M. E., C. Ebenau-Jehle, A. Zaar, and G. Fuchs.** 2001. Reinvestigation of a new type of aerobic benzoate metabolism in the proteobacterium *Azoarcus evansii*. J. Bacteriol. **183:**1899–1908.
27. **Olivera, E. R., B. Minabers, B. Garcia, C. Muniz, M. A. Moreno, A. Ferrandez, E. Diaz, J. L. Garcia, and J. M. Luengo.** 1998. Molecular chracterization of the phenylacetic acid catabolic pathway in *Pseudomonas putida* U: the phenylacetyl-CoA catabolon. Proc. Natl. Acad. Sci. USA **95:**6419–6424.
28. **Park, S. J., and S. Y. Lee.** 2003. Identification and characterization of a new enoyl coenzyme A hydratase involved in the biosynthesis of medium-chain-length polyhydroxyalkanoates in recombinant *Escherichia coli*. J. Bacteriol. **185:**5391–5397.
29. **Perozich, J., I. Kuo, R. Lindahl, and J. Hempel.** 2001. Coenzyme specificity in aldehyde dehydrogenase. Chem. Biol. Interact. **130–132:**115–124.
30. **Perozich, J., H. Nicholas, R. Lindahl, and J. Hempel.** 1999. The big book of aldehyde dehydrogenase sequences. An overview of the extended family. Adv. Exp. Med. Biol. **463:**1–7.
31. **Sambrook, J., E. F. Fritsch, and T. Maniatis.** 1989. Molecular cloning: a laboratory manual, 2nd ed. Cold Spring Harbor Laboratory Press, Cold Spring Harbor, N.Y.
32. **Schachter, D., and J. V. Taggart.** 1976. Benzoyl coenzyme A and hippurate synthesis. J. Biol. Chem. **203:**925–933.
33. **Schuehle, K., M. Jahn, S. Ghisla, and G. Fuchs.** 2001. Two similar gene clusters coding for the enzymes of a new type of aerobic 2-aminobenzoate (anthranilate) metabolism in the bacterium *Azoarcus evansii*. J. Bacteriol. **183:**5268–5378.
34. **Steinmetz, C. G., P. Xie, H. Weiner, and T. D. Hurley.** 1997. Structure of mitochondrial aldehyde dehydrogenase: the genetic component of ethanol aversion. Structure **5:**701–711.
35. **Torres, R. A., and T. C. Bruice.** 1999. Sigmatropic hydrogen migration in the mechanism of oxidation of 2-aminobenzoyl-CoA by 2-aminobenzoyl-CoA monooxygenase/reductase. Proc. Natl. Acad. Sci. USA **96:**14748–14752.
36. **Vedadi, M., A. Vrielink, and E. Meighen.** 1997. Involvement of conserved glycine residues, 229 and 234, of *Vibrio harveyi* aldehyde dehydrogenase in activity and nucleotide binding. Biochem. Biophys. Res. Commun. **238:**448–451.
37. **Vedadi, M., R. Szittner, L. Smillie, and E. Meighen.** 1995. Involvement of cysteine 289 in the catalytic activity of an NADP(+)-specific fatty aldehyde dehydrogenase from *Vibrio harveyi*. Biochemistry **34:**16725–16732.
38. **Wang, X., and H. Weiner.** 1995. Involvement of glutamate 268 in the active site of human liver mitochondrial (class 2) aldehyde dehydrogenase as probed by site-directed mutagenesis. Biochemistry **34:**237–243.
39. **Weiner, H., J. Farres, U. J. Rout, X. P. Wang, and C. F. Zheng.** 1995. Site directed mutagenesis to probe for active site components of liver mitochondrial aldehyde dehydrogenase, p. 1–7. *In* H. Weiner, R. S. Holmes, and B. Wermuth (ed.), Enzymology and molecular biology of carbonyl metabolism, vol. 5. Plenum Press, New York, N.Y.
40. **Zaar, A., J. Gescher, W. Eisenreich, A. Bacher, and G. Fuchs.** 2004. New enzymes involved in aerobic benzoate metabolism in *Azoarcus evansii*. Mol. Microbiol. **54:**223–238.
41. **Zaar, A., W. Eisenreich, A. Bacher, and G. Fuchs.** 2001. A novel pathway of aerobic benzoate catabolism in the bacteria *Azoarcus evansii* and *Bacillus stearothermophilus*. J. Biol. Chem. **276:**24997–25004.
42. **Zehr, B. D., T. J. Savin, and R. E. Hall.** 1989. A one-step, low background Coomassie staining procedure for polyacrylamide gels. Anal. Biochem. **182:** 157–159.
43. **Zhang, L., B. Ahvazi, R. Szittner, A. Vrielink, and E. Meighen.** 2000. A histidine residue in the catalytic mechanism distinguishes *Vibrio harveyi* aldehyde dehydrogenase from other members of the aldehyde dehydrogenase superfamily. Biochemistry **39:**14409–14418.